Hindawi
Adsorption Science & Technology
Volume 2023, Article ID 9922446, 11 pages
https://doi.org/10.1155/2023/9922446

Research Article

Sonicating for the Uptake of Paracetamol from Solution by Activated Carbon from Oak: Kinetics, Thermodynamics, and Isotherms

Alaa M. Al-Ma'abreh,[1] **Gada Edris**,[1] **and Mike Kh. Haddad**[2]

[1]*Department of Chemistry, Faculty of Science, Isra University, P.O. Box 22, Amman 11622, Jordan*
[2]*Department of Renewable Energy Engineering, Faculty of Engineering, Isra University, P.O. Box 22, Amman 11622, Jordan*

Correspondence should be addressed to Alaa M. Al-Ma'abreh; alaa.almaabreh@iu.edu.jo

Received 6 January 2023; Revised 17 February 2023; Accepted 20 February 2023; Published 3 March 2023

Academic Editor: Sami-ullah Rather

This inquiry used ultrasonic waves to uptake paracetamol (PA) by using oak-based activated carbon (ACO). The surface of ACO was explored based on FT-IR, SEM, and XRD before and after the adsorption. The kinetic data for PA adsorption onto ACO corresponds to a pseudo-second-order kinetic model. Isothermal models of the Langmuir, Freundlich, D-R, and Temkin were used. The adsorption of PA onto ACO was found to be a monolayer with 96.03% uptake, which corresponds to Langmuir. The thermodynamic experiments revealed the endothermic nature of PA adsorption onto ACO. Under the investigated optimal conditions, the adsorption capacity of PA onto ACO was found to be 97.1 mg. L^{-1}. ACO could be recycled after six regenerations. Ultimately, sonicating has adequate performance for the uptake of PA by ACO.

1. Introduction

Hazardous material pollution has recently grown into a significant concern throughout the world. Recent research has focused on the efficient removal of such contaminants to reduce the threat that they pose to living organisms [1]. Diverse forms of organic pollutants, such as pharmaceuticals, were detected in a wide range of water supplies. Since pharmaceuticals are essential to preserving human and animal health, their production has grown significantly in recent decades. These pharmaceutical compounds are regularly released in enormous quantities into the environment, mainly through water and soil, from a diversity of sources, including anthropogenic activities, the pharmaceutical industry, and hospitals [2]. Due to its efficacy in relieving pain and fever, paracetamol, also known as acetaminophen (Scheme 1), is one of the most used medications globally. Because of its solubility and hydrophilicity, paracetamol concentrates readily in water. Paracetamol decomposes gradually in the environment since it is not biodegradable [2]. Paracetamol is particularly toxic to the liver, posing a risk of hepatitis development [3]. In the past, significant efforts were made to improve water treatment processes. As a result, many effective techniques for discarding pharmaceutical micropollutants from polluted water were developed.

Various techniques were employed for removing pollutants from water, such as filtration, chemical precipitation, coagulation, ion exchange, ozonation, advanced oxidation, reverse osmosis, biodegradation, and adsorption processes [4]. Adsorption is a broadly used technique for removing pollutants from water due to its exceptional

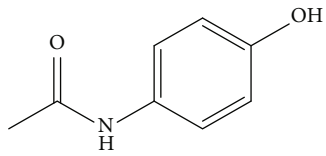

Scheme 1: Paracetamol (acetaminophen) $C_9H_8NO_2$.

efficiency, low toxicity, modesty, environment-friendly, nondestructiveness, and insignificant cost [5]. The most prominent adsorbent for extracting contaminants, specifically from water, is activated carbon due to its adaptability and attractive characteristics, such as its high surface area, porosity, and distinct chemical properties, which enable interaction with various chemical substances [6]. Activated carbon has been prepared using a variety of precursors in frequent studies. Among these precursors is oak fruit. Oak (Quercus calliprinos) is a prevalent plant in the Eastern Mediterranean, growing on rocky hillsides. It is indigenous to Jordan and can be found in Salt, Ajlun, Jerash, Amman, Tafila, and Shobak. The fruit of the oak is a nut called an acorn that grows in a cup-like structure (called a cupule). In many investigations, the uptake of paracetamol from aqueous solutions by adsorption onto activated carbon was performed based on the shaking technique assisted with sonication. Also, numerous studies used modified activated carbon such that modified by aminoterphthalic acid [7]. Sonication boosted the migration of pollutants into activated carbon pores, causing higher efficiency [8].

The aim of this study is to prove the effectiveness of using just sonication in removing paracetamol from an aqueous solution and simulated samples. Numerous variables, including adsorbent dose, initial concentration, contact time, and pH, were examined for their effectiveness. The equilibrium and mechanism of the adsorption process were examined by kinetic and isothermal investigations.

2. Materials and Methods

2.1. Reagents and Instruments. Paracetamol with a purity of >99% (Scheme 1) was acquired from Sigma Aldrich and used without any more cleansing. This analgesic was chosen for its widespread production and consumption around the world. Calculated amounts of powder standards from PA were dissolved in distilled water to prepare stock solutions (250 mg. L^{-1}). The prepared solutions were kept out of the light at 4°C. Operative concentrations (10–100 mg L^{-1}) were prepared from stock solutions by dilution. Solutions of 0.1 M NaOH and 0.1 M HCl were employed for pH adjustment. FT-IR instrument (TENSOR from Bruker) was employed for the functional groups evident on the activated carbon surface and their implications in the adsorption. The LEO 1550 scanning electron microscopy (SEM) was employed to obtain images of the adsorbent surface. X-ray diffraction patterns were obtained from an XRD D5005 diffractometer (Siemens, Munich, Germany).

2.2. Preparation and Characterization of Adsorbent. The abundant oak cupule was collected as waste from the north of Jordan in the summer. Subsequently, the oak cupule was repeatedly rinsed with distilled water, dried at 80°C for 48 hours, and then crushed. The crushed sample was used to prepare activated carbon according to the method [9]. The prepared activated carbon was ground and sieved to obtain particles of 180 μm particle size. Finally, the prepared activated carbon was stored in a desiccator and employed for paracetamol uptake.

2.2.1. Characterization of ACO. The surface morphology of ACO was explored using techniques of scanning electron microscopy (SEM), Fourier transform infrared (FT-IR), and X-ray diffraction (XRD).

2.2.2. Bach Adsorption Experiment. All experiments were performed using a laboratory ultrasonic water bath (Branson 5800, USA). Each experiment was performed three times. A 50.0 mL of PA solution at different concentrations was added to a weighed amount of ACO into a 250 ml of the Erlenmeyer flask. The mixtures were sonicated for a particular time. The mixtures were filtered and subjected to absorbance measurements to determine the concentration. The effects of sonication time, initial PA concentration, adsorbent dose, solution pH, and temperature were investigated. A UV-6100 PC double-beam spectrophotometer was used to investigate the PA concentrations at a wavelength of 244 nm. The adsorbed amount of PA onto the ACO, q_e (mg. g^{-1}), was calculated using Equation (1) [10, 11].

$$q_e = \frac{(C_i - C_{\text{eq}})V}{m}. \tag{1}$$

q_e (mg. g^{-1}) is the adsorbed PA amount at equilibrium, C_i (mg. L^{-1}) is the initial Pa concentration, C_{eq} (mg. L^{-1}) are the equilibrium PA concentration, and V (L) is the volume of working solution.

The removal percentage was calculated based on Equation (2).

$$\%\text{Removal} = \frac{(C_i - C_{\text{eq}})}{C_{\text{eq}}} \times 100. \tag{2}$$

3. Results and Discussion

3.1. Characterization of Adsorbent

3.1.1. FT-IR Analysis. FT-IR analysis (Figure 1) was performed for ACO adsorbent and ACOPA (the coated ACO with paracetamol after the adsorption process). The results revealed the existence of various functional groups. Results were summarized in Table 1 [9]. As a result, there are obvious shifts in absorbance and changes in intensity confirm the adsorption of PA onto ACO.

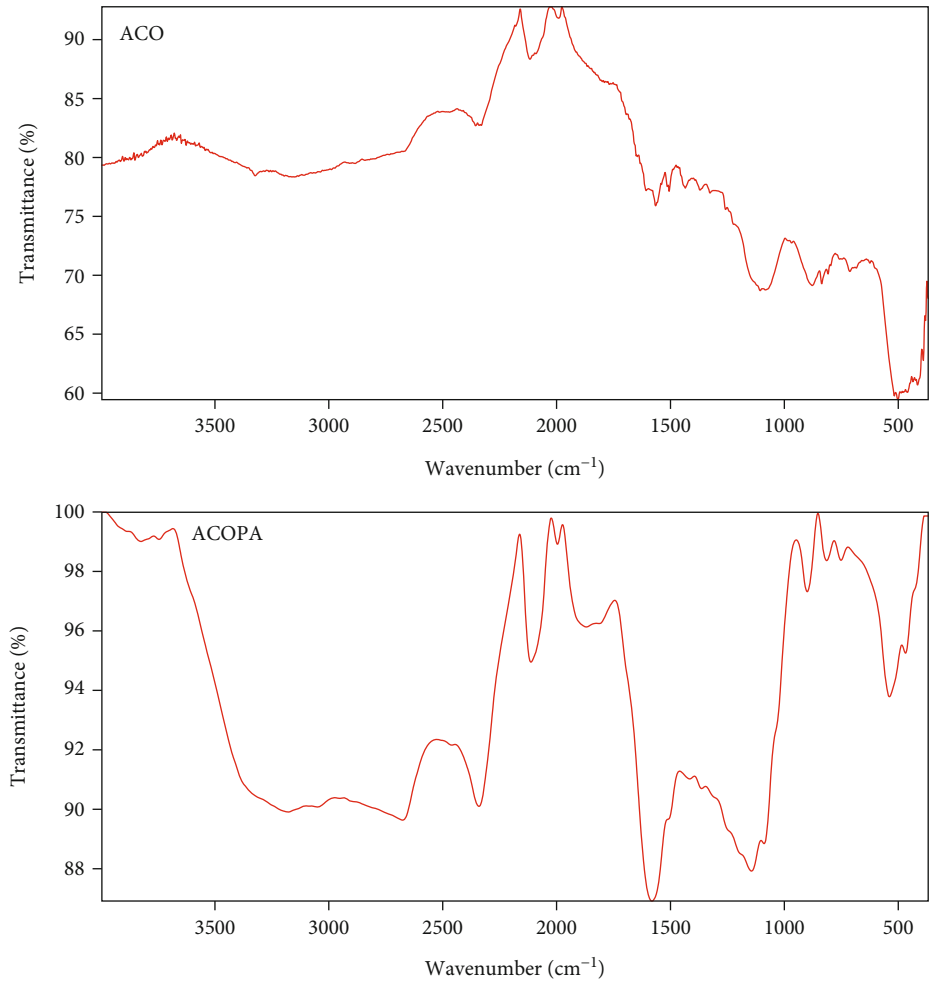

Figure 1: FT-IR analysis of ACO and ACOPA.

Table 1: FTIR results.

	ACO cm^{-1}	ACOPA cm^{-1}
O–H stretching vibration	3323.28	3178.59
Aliphatic C-H group stretching vibrations of the alkyl groups	2885.00	2675.86
Stretching vibration of olefins carbonyl groups (C=O) in conjugated compounds	1607.06	1812.94
Carboxylic/aromatic hydroxyl (–OH) stretching of the phenol group	1565.43	1581.35
Stretching vibration of aromatic skeletal	1505.78	1498.35
Bending vibration of aromatic C–H out-of-plane	877.81 & 712.32	899.57 & 750.34
Stretching in C–C vibrations	459.18	468.19

3.1.2. SEM Analysis of Adsorbent Material. Figures 2(a) and 2(b) show SEM images of the surface morphology of ACO adsorbent and ACOPA after paracetamol adsorption. The distinct difference between the two images, as well as the aggregates recognizable in Figure 2(b), confirm the paracetamol adsorption onto the ACO surface.

3.1.3. XRD Analysis of Adsorbent Material. The crystallographic structure of ACO and ACOPA was determined using XRD analysis. The obtained spectra are depicted in Figure 3. The obvious changes in intensity and peak broadening confirm the accumulation of PA onto the ACO.

3.2. Batch Adsorption

3.2.1. Influence of Adsorbent Dosage. The effectiveness of the adsorption process is strongly affected by the adsorbent dosage. In this study, the dosage of ACO varied from

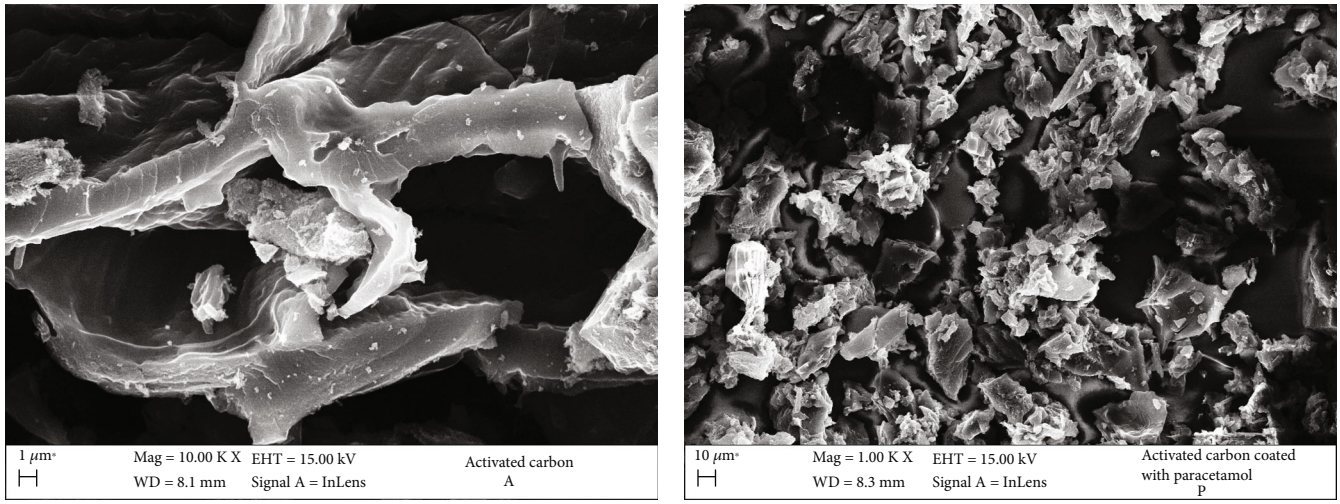

(a) (b)

Figure 2: SEM analysis of (a) ACO and (b) ACOPA.

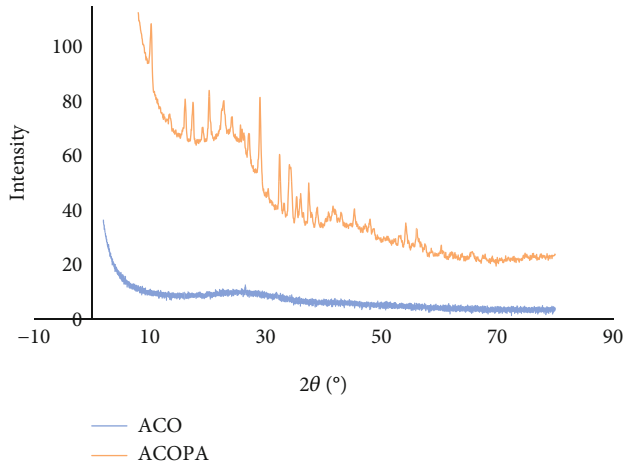

Figure 3: XRD analysis of ACO and ACOPA.

10 to 100 mg. At 25 ± 1°C for 60 minutes, a volume of 50.0 ml of 50 mg/L L^{-1} PA solution with a pH of 7.0 was sonicated with a specific dose of ACO. Figure 4 shows that the proportion of paracetamol removed increases when the ACO dose is increased due to the plentiful presence of active sites at the initial stages of the adsorption process. At 50.0 mg, the increments in the uptake become very slight, signifying that the optimum dose of ACO for the removal of PA from an aqueous solution by sonication has already been achieved.

3.2.2. Influence of Sonication Time. Contact time (sonicating) was one of the factors that had a significant impact on the effectiveness of the adsorption process. The batch adsorption experiments were conducted by sonication of 50 mg ACO with 50 ml of 50 mg, L^{-1} PA concentration at 7.0 pH, and 25 ± 1°C for 15-120 minutes. Figure 5 shows the adsorption equilibrium of PA onto the ACO surface was reached after 60 min, and then the uptake becomes approximately constant.

3.2.3. Influence of PA Initial Concentration. Figure 6 demonstrates how the initial concentration of the adsorbate substantially impacts the adsorption of PA onto ACO. In this study, the initial concentration of PA varied from 10 to 90 mg. L^{-1}. In the first stages, the change in adsorption is likely to be negligible until it reaches 50 mg. L^{-1} due to the availability of achievable active sites. After the optimal initial concentration (50 mg. L^{-1}), the uptake starts to drop due to the saturation of active sites with PA molecules.

3.2.4. Influence of pH. The pH of the solution is a crucial parameter in the adsorption process. Firstly, the value of pHpzc was determined by shaking 150 mg of ACO adsorbent with 50.0 ml of 0.1 M NaOH solution for 24 hours at a pH of 2, 4, 6, 8, 10, and 12. Figure 7 shows the pHpzc is equal to 6.39. For pH values exceeding pHpzc, the adsorbent surface of ACO becomes negative, whereas, for values beneath pHpzc, it becomes positive [12].

In this study, the impact of pH on the adsorption of PA onto ACO was investigated at a temperature of 25 ± 1°C, an initial concentration of 50 mg. L^{-1} and ACO dosage of 50 mg, sonication time for 60 min, and pH ranged from 3-11. Scheme 2 illustrates the protonated and deprotonated structures of PA.

The optimal adsorption of PA onto ACO was recorded at pH 5.0, as Figure 8 shows. Adsorption was maximal at an acidic pH because the phenols continued to remain undissociated, and the interactions between the ACO adsorbent and the PA were issued. Equilibrium was achieved at pH 7.0, then rapidly deteriorated beyond pH 9.0 as a result of the repulsion between the negatively charged ACO surface and the anionic (deprotonated) paracetamol [13].

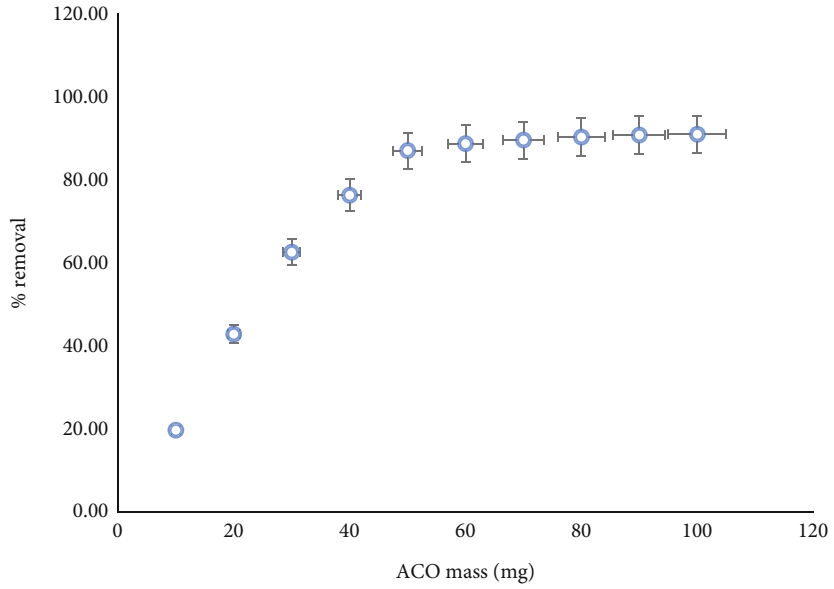

FIGURE 4: Influence of adsorbent dosage on the adsorption of PA onto ACO (dosage = 10 – 100 mg, C_i = 50 mg. L^{-1}; pH = 7.0, sonication time = 60 min, and $T = 25 \pm 1^{\circ}C$).

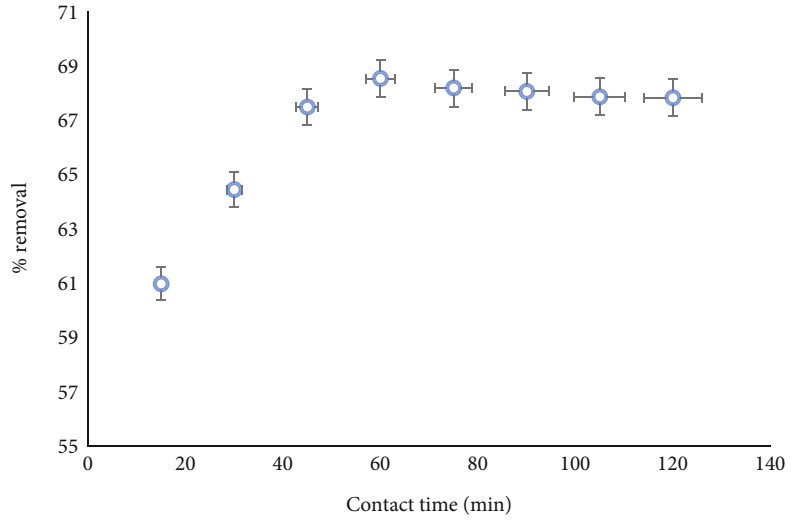

FIGURE 5: Influence of contact time on the adsorption of PA onto ACO (dosage = 50 mg, C_i = 50 mg. L^{-1}; pH = 7.0, sonication time = 15 – 120 min, and $T = 25 \pm 1^{\circ}C$).

3.3. Adsorption Kinetic and Mechanism. The kinetics and the mechanism of PA adsorption onto ACO were investigated using pseudo-first-order, pseudo-second-order, and intraparticle diffusion kinetics models. Plotting kinetic data according to Equations (3) and (4) [14] determines whether the PA adsorption onto ACO was first or second order. Results in Figure 9 indicate that the process is of pseudo-second order with an R^2 of 0.9928 and a rate constant (k_1) of 0.0287 g. mg^{-1}. min^{-1}.

$$q_t = q_e\left(1 - e^{-k_1 t}\right)t, \tag{3}$$

$$q_t = \frac{q_e^2 k_2 t}{q_e k_2 t + 1}, \tag{4}$$

q_e is the equilibrium amount of adsorbate per unit mass of adsorbent (mg. g^{-1}), q_t is the equilibrium amount of adsorbate per unit mass of adsorbent at time t (mg. g^{-1}), and k_1 and k_2 are the rate constant in min^{-1} and g. mg^{-1}. min^{-1}, respectively.

The intraparticle diffusion model represented by Equation (5) was employed for the demonstration of PA adsorption onto the ACO mechanism [15].

$$q_t = K_{id}t^{1/2} + C, \tag{5}$$

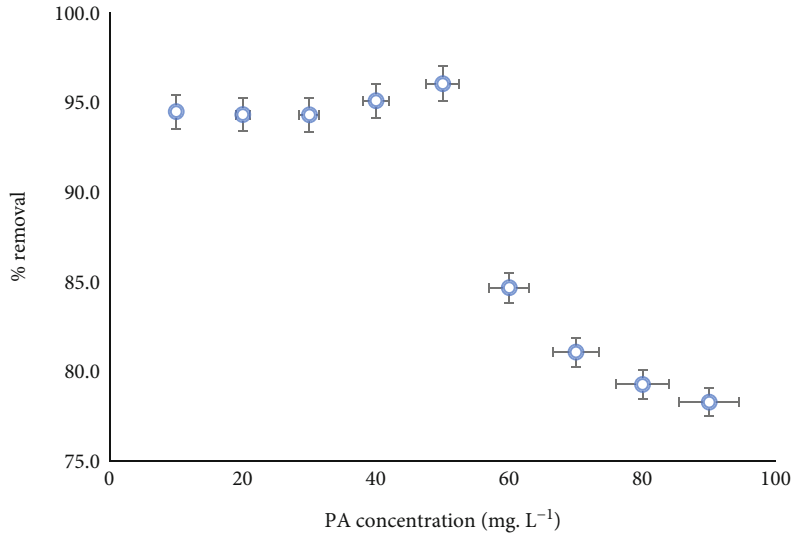

FIGURE 6: Influence of PA initial concentration on the adsorption onto ACO (dosage = 50 mg, C_i = 10 – 90 mg. L^{-1}; pH = 7.0, sonication time = 60 min, and $T = 25 \pm 1^{\circ}C$).

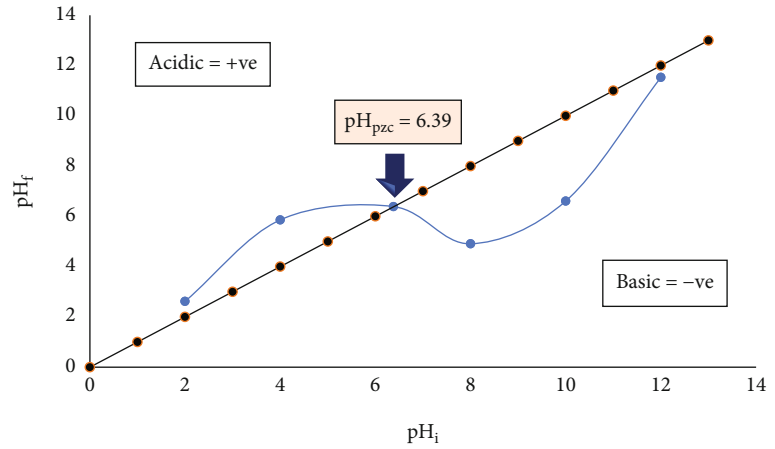

FIGURE 7: pH_{pzc} for ACO.

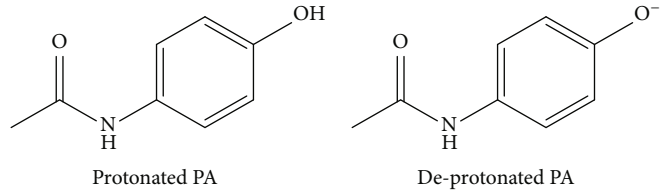

SCHEME 2: Paracetamol (acetaminophen) structures in acidic and basic solution.

where q_t is the adsorbate amount (mg. g^{-1}), K_{id} is the rate constant (mg. g^{-1}. $min^{-0.5}$), and $t^{1/2}$ is the square root of time ($min^{0.5}$). It is anticipated that if the intercept C equals zero, intraparticle diffusion would be the only rate-limiting step. The effect of surface adsorption rises in significance when the C constant is raised. According to Figure 10, the rate-limiting step is surface adsorption, not intra-particle diffusion.

Table 2 summarized the R^2 and constants for kinetics models.

3.4. Adsorption Isotherms. Adsorption isotherms play a crucial role in elucidating the interaction between the adsorbate molecules and the adsorption sites on the surface. Isothermal models Langmuir, Freundlich, Temkin, and Dubinin-Radushkevich (D-R) isothermal models were

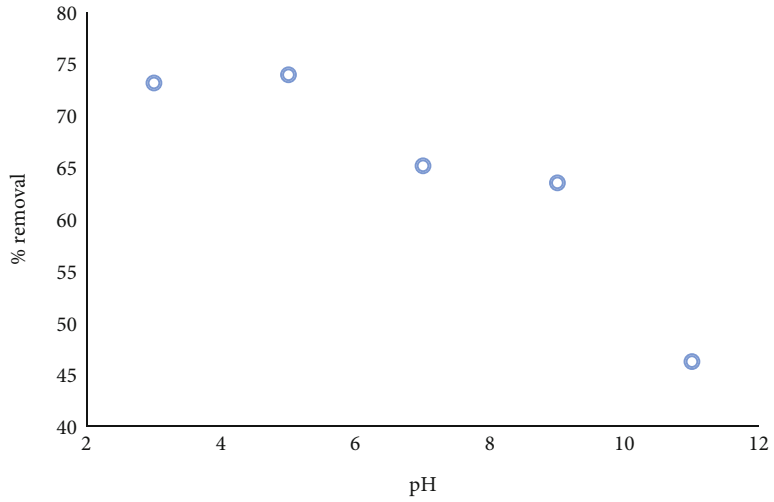

Figure 8: Influence of pH on the adsorption of PA onto ACO (dosage = 50 mg, C_i = 50 mg.L^{-1}, pH = 3 – 11, sonication time = 60 min, and $T = 25 \pm 1^{\circ}C$).

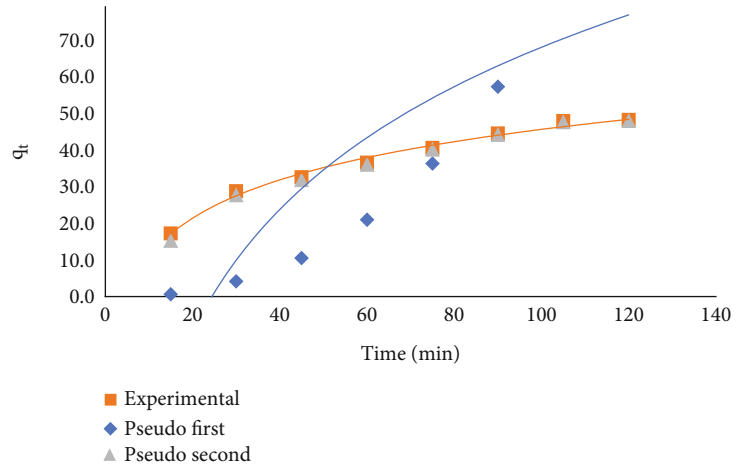

Figure 9: Kinetic studies of PA adsorption onto ACO (dosage = 50 mg, C_i = 50 mg.L^{-1}, pH = 7, sonication time = 10 – 120 min, and T = 25 ± 1 ∘ C).

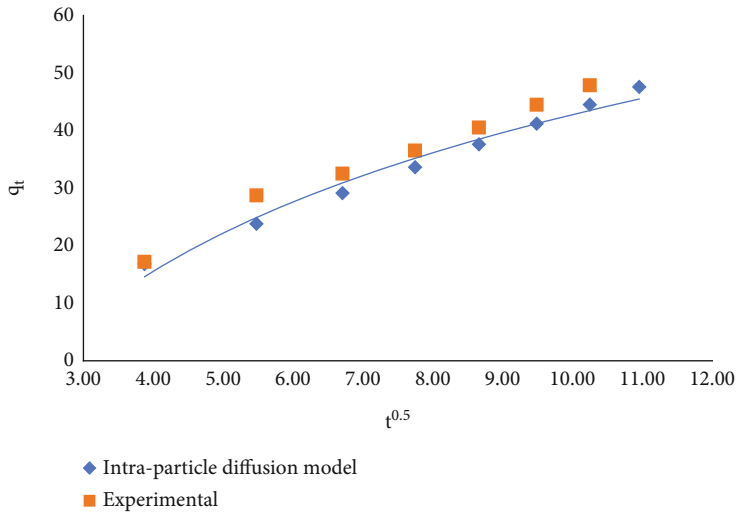

Figure 10: Intraparticle Diffusion model for Pa adsorption onto ACO.

Table 2: Kinetics constants.

First order kinetics		Second order kinetics		Intraparticle diffusion	
R^2	K_1 (min^{-1})	R^2	K_2 ($g.mg^{-1}\ min^{-1}$)	R^2	K_{id} ($mg.\ g^{-1}.\ Min^{-0.5}$)
0.7749	1.6×10^{-3}	0.9928	2.78×10^{-2}	0.9771	0.4346

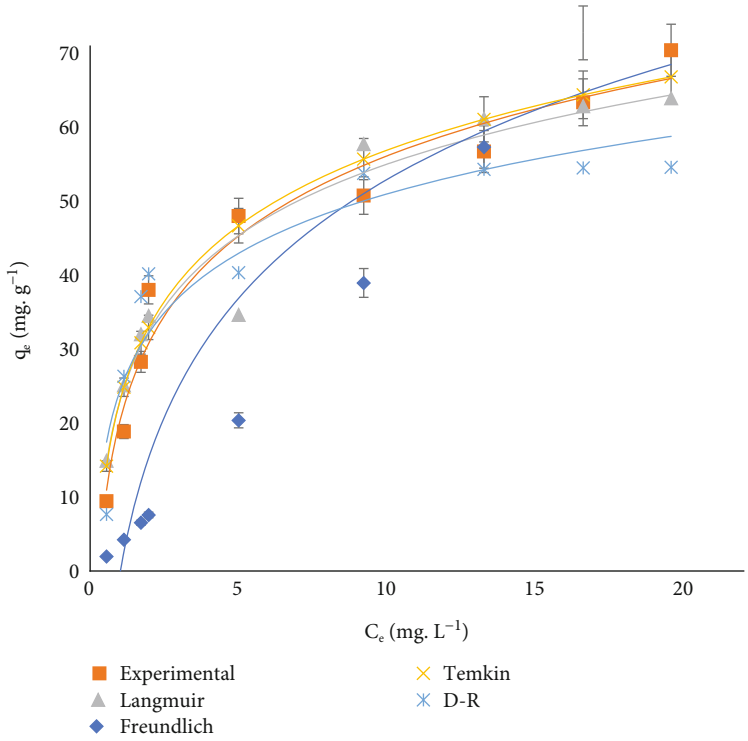

Figure 11: Langmuir, Freundlich, Temkin, and D-R isotherms of PA adsorption onto ACO.

employed to elucidate the adsorption mechanism of PA onto ACO. Equations (6), (7), (8), and (9) represent the nonlinear form of the Langmuir, Freundlich, Temkin, and Dubinin-Radushkevich (D-R) isotherm models, respectively [10, 11].

$$q_e = \frac{k_L q_m C_e}{(1 + k_L C_e)}, \tag{6}$$

$$q_e = K_F C_e^{1/n}, \tag{7}$$

$$q_e = B \ln A C_e, \tag{8}$$

$$q_e = q_m e^{-B_D \varepsilon^2}. \tag{9}$$

q_e is the equilibrium adsorbate amount (mg. g^{-1}), q_e is the equilibrium adsorbate amount (mg. g^{-1}), C_e is the equilibrium adsorbate concentration (mg. L^{-1}), k_L, the Langmuir isotherm constant, is associated to adsorption energy and utilized to determine adsorbate affinity to the adsorbent surface, q_m is the adsorption capacity (mg. g^{-1}), K_F is the Freundlich isotherm constant (mg. g^{-1}), n is the adsorption intensity, A is the binding constant in g^{-1} at equilibrium, B is constant associated to the adsorption heat, B_D is the D-R constant mol^2/KJ^2, and $\mathcal{E}$ (Polanyi potential) in D-R isotherm and the mean energy of the adsorption (KJ. Mol^{-1}) could be obtained using Equations (10) and (11), respectively.

Table 3: Isotherms model constants.

Isotherm	Isotherms constants	
Langmuir	R_L^2	0.9476
	K_L	0.05
	q_m, mg. g-1	138
Freundlich	R_F^2	0.7880
	K_F, mg/g	20.28
	n	2.26
Temkin	R^2	0.8904
	B	14.8
	A	4.7
D-R	R^2	0.897
	B_D, $mol^2.KJ^{-2}$	3×10^{-7}
	E, KJ/Mol	1.3

$$\varepsilon = RT \ln\left(1 + \frac{1}{C_e}\right), \tag{10}$$

Table 4: Thermodynamic parameters of PA adsorption onto ACO.

Adsorbent	T (K)	q_m (mg. g^{-1})	Thermodynamic parameters		
			ΔG° (KJ Mol^{-1})	ΔH^o (KJ Mol^{-1})	ΔS° (KJ $K^{-1}Mol^{-1}$)
ACO	298	80.65	15.958	36.442	0.0697
	308	77.45	14.345		
	318	62.13	14.604		

$$E = \frac{1}{\sqrt{2B_D}}. \quad (11)$$

Figure 11 demonstrates the results of the fourth isotherms. Correlation coefficients (R^2), dimensional factors, and associated constants were presented in Table 3. R^2 values determined that the Langmuir isotherm properly appropriately characterized the PA adsorption onto ACO, indicating monolayer and homogenous adsorption. The value of the Temkin constant (B) (Table 3), reveals that the PA adsorption onto the ACO adsorbent is endothermic. In accordance with the D-R isotherm, the predicted energy values, 1.3 KJ<8.0 KJ. Mol^{-1} imply the physisorption nature of PA onto ACO [16].

3.5. Thermodynamics. Thermodynamic parameters ΔG°, ΔH°, and ΔS° were assessed to evaluate the efficiency of PA adsorption onto ACO (Table 4). The slope and intercept of the plot of ln (K_L) versus 1/T (K^{-1}) were used to get the enthalpy change ΔH^o (kJ mol^{-1}) and entropy change ΔS^o (J/mol^{-1} K^{-1}) of PA adsorption, respectively. The Gibbs free energy, ΔG°, was calculated using Equation (12), enthalpy, ΔH°, and entropy, ΔS° was possible to calculate using Equation (13) (Van't Hoff's).

$$\Delta G^\circ = -RTln(K_L), \quad (12)$$

$$\ln(K_L) = \frac{\Delta S^\circ}{R} - \frac{\Delta H^\circ}{T}\left(\frac{1}{T}\right). \quad (13)$$

K_L is a dimensionless and represent the adsorption equilibrium constant according to the best-fitted model. R is the universal constant of ideal gases, 8.314 J•K^{-1} mol^{-1}. For PA adsorption onto ACO, positive values of Gibb's free energy (ΔG°) indicate that the process is not spontaneous. The positive value of enthalpy (ΔH^o) confirms the endothermic nature of the adsorption process. Enthalpy magnitude indicates physisorption through the van der Waals if less than 20 kJ mol^{-1} or electrostatic forces between PA and ACO if between 20 and 80 kJ mol^{-1} [17]. Positive entropy change (ΔS^o) values suggest adsorbate/adsorbent interface unpredictability and ACO adsorbent affinity [18]. Thermodynamic experiments were performed under the same experimental conditions previously applied in the adsorption equilibrium; thus, under temperature variation (25 ± 1°C, 35 ± 1°C, and 45 ± 1°C) and sonication for 60 min.

3.6. Simulated Sample. A tablet of three commercial medicines containing PA was dissolved in tap water and sonicated with 50 mg ACO for 60.0 min under optimal conditions. The PA uptake was found to be 81.78%, 84.27%, and 83.12%, confirming the effectiveness of ACO in the uptake of PA by sonication.

Table 5: Comparison of PA adsorption onto ACO with other reported adsorbents.

Adsorbent	q_{max} (mg. g^{-1})
Commercial AC [19]	101
Olive stones AC [20]	100
Tea waste AC [21]	99.42
Brazil nutshells AC [22]	306.7
Butia capitata endocarp AC [23]	100.60
plant sludge of the beverage industry AC [24]	145
Ceramic AC [25]	159
Cannabis sativum Hemp AC [26]	16.18
Fruit of Butiacapitate AC [27]	98.19
Oak cupule AC (present study)	97.91

4. Comparison with Other Activated Carbon Adsorbents

The maximum PA uptake capacities by ACO based on sonication was compared to other activated carbon adsorbent based on the shaking technique (Table 5). The comparison shows that ACO has an adsorption capacity of 97.91 mg g^{-1} near to many of the other reported adsorbents.

5. Desorption and Regeneration Study

Sodium hydroxide is found to be the best for the regeneration of PA adsorbed [28]. 1.0 M of NOH was used for the elution of PA from the ACO surface. The percentage of desorption was calculated using Equation (14).

$$\%\text{Desorption} = \frac{C_{de}}{C_{ad}} \times 100, \quad (14)$$

whereas PA is represented by the desorbed concentration (C_{de}) and the adsorbed concentration (C_{ad}). The regenerated PA as a percentage of desorption was found to be 63.2% after six cycles as elucidated in Figure 12.

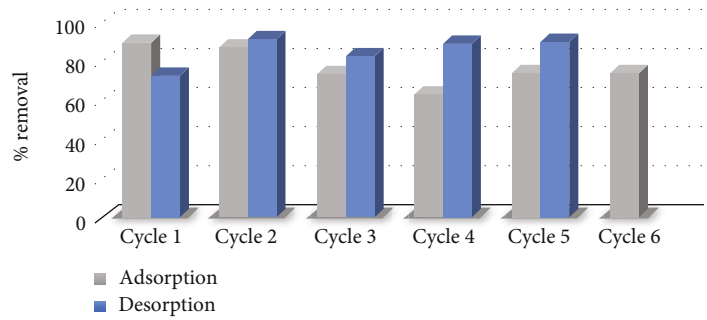

Figure 12: Regeneration of ACO adsorbent.

6. Conclusion

This study revealed that the PA is successfully uptake from an aqueous solution and simulated sample by activated carbon prepared from an oak cupule (ACO) by solely sonication. The experimental results demonstrated that the adsorption potential of PA onto ACO adsorbent is adversely impacted by operative factors such as sonication time, pH, adsorbent dose, temperature, and PA initial concentration. Maximum uptake (96.03%) of 50 mg g^{-1} PA was achieved after 60 minutes of sonication with 50 mg ACO at 45°C and 5.0 pH. The adsorption isotherm data best fit the Langmuir model. Information from the kinetic studies indicated that the pseudo-second-order kinetic model was in better agreement compared to the pseudo-first-order kinetic. Thermodynamically, the adsorption of PA onto ACO was found to be endothermic and nonspontaneous. ACO could be reused after six cycles with decrease in efficiency by 14.89%.

Data Availability

The data that support the findings of this study are available from the corresponding author upon reasonable request.

Conflicts of Interest

The authors declare that they have no known competing financial interests or personal relationships that could have appeared to influence the work reported in this paper.

Authors' Contributions

All authors contributed to the study conception and design. Material preparation, data collection, and analysis were performed by all authors (Alaa Mahmoud Al-Ma'abreh, Gada Idris, and Mike Haddad). The first draft of the manuscript was written by Alaa Mahmoud Al-Ma'abreh, and all authors commented on previous versions of the manuscript. All authors read and approved the final manuscript.

References

[1] A. Jahanban-Esfahlan, R. Jahanban-Esfahlan, M. Tabibiazar, L. Roufegarinejad, and R. Amarowicz, "Recent advances in the use of walnut (*Juglans regia* L.) shell as a valuable plant-based bio-sorbent for the removal of hazardous materials," *RSC Advances*, vol. 10, no. 12, pp. 7026–7047, 2020.

[2] R. C. Ferreira, "Effect of solution pH on the removal of paracetamol by activated carbon of dende coconut mesocarp," *Chemical and Biochemical Engineering Quarterly Journal*, vol. 29, pp. 47–53, 2015.

[3] S. Gong, T. Lan, L. Zeng et al., "Gut microbiota mediates diurnal variation of acetaminophen induced acute liver injury in mice," *Journal of Hepatology*, vol. 69, no. 1, pp. 51–59, 2018.

[4] C. A. Igwegbe, C. O. Aniagor, S. N. Oba et al., "Environmental protection by the adsorptive elimination of Acetaminophen from water: a comprehensive review," *Journal of Industrial and Engineering Chemistry*, vol. 104, pp. 117–135, 2021.

[5] S. Babel and T. A. Kurniawan, "Low-cost adsorbents for heavy metals uptake from contaminated water: a review," *Journal of Hazardous Materials*, vol. 97, no. 1-3, pp. 219–243, 2003.

[6] C. Jung, A. Son, N. Her, K. Zoh, J. Cho, and Y. Yoon, "Removal of endocrine disrupting compounds, pharmaceuticals, and personal care products in water using carbon nanotubes: a review," *Journal of Industrial and Engineering Chemistry*, vol. 27, pp. 1–11, 2015.

[7] A. M. Aldawsari, I. H. Alsohaimi, A. A. Al-Kahtani, A. A. Alqadami, Z. E. A. Abdalla, and E. A. M. Saleh, "Adsorptive performance of aminoterephthalic acid modified oxidized activated carbon for malachite green dye: mechanism, kinetic and thermodynamic studies," *Separation Science and Technology*, vol. 56, no. 5, pp. 835–846, 2021.

[8] Y. Wu, Y. Han, Y. Tao et al., "Ultrasound assisted adsorption and desorption of blueberry anthocyanins using macroporous resins," *Ultrasonics Sonochemistry*, vol. 48, pp. 311–320, 2018.

[9] J. Bedia, M. Peñas-Garzón, A. Gómez-Avilés, J. Rodriguez, and C. Belver, "A review on the synthesis and characterization of biomass-derived carbons for adsorption of emerging contaminants from water," *Journal of Carbon Research*, vol. 4, no. 4, p. 63, 2018.

[10] A. M. Al-Ma'abreh, R. A. Abuassaf, D. A. Hmedat, M. Al Khabbas, S. Awaideh, and G. Edris, "Comparative study for the removal of crystal violet from aqueous solution by natural biomass adsorbents of a pinecone, cypress, and oak: kinetics, thermodynamics, and isotherms," *Desalination and Water Treatment*, vol. 274, pp. 245–260, 2022.

[11] A. M. Al-Ma'abreh, R. A. Abuassaf, D. A. Hmedat et al., "Adsorption characteristics of hair dyes removal from aqueous solution onto oak cupules powder coated with ZnO," *International Journal of Molecular Sciences*, vol. 23, no. 19, article 11959, 2022.

[12] Y. Sun, H. Li, G. Li, B. Gao, Q. Yue, and X. Li, "Characterization and ciprofloxacin adsorption properties of activated carbons prepared from biomass wastes by H_3PO_4 activation," *Bioresource Technology*, vol. 217, pp. 239–244, 2016.

[13] V. Bernal, A. Erto, L. Giraldo, and J. Moreno-Piraján, "Effect of solution pH on the adsorption of paracetamol on chemically modified activated carbons," *Molecules*, vol. 22, no. 7, p. 1032, 2017.

[14] N. S. Kumar, M. Asif, and M. I. Al-Hazzaa, "Adsorptive removal of phenolic compounds from aqueous solutions using pine cone biomass: kinetics and equilibrium studies," *Environmental Science and Pollution Research*, vol. 25, no. 22, pp. 21949–21960, 2018.

[15] R. Lafi, I. Montasser, and A. Hafiane, "Adsorption of congo red dye from aqueous solutions by prepared activated carbon with oxygen-containing functional groups and its regeneration," *Adsorption Science & Technology*, vol. 37, no. 1-2, pp. 160–181, 2019.

[16] E. Malkoc and Y. Nuhoglu, "Fixed bed studies for the sorption of chromium(VI) onto tea factory waste," *Chemical Engineering Science*, vol. 61, no. 13, pp. 4363–4372, 2006.

[17] G. R. Mahdavinia, F. Bazmizeynabad, and B. Seyyedi, "Kappa-Carrageenan beads as new adsorbent to remove crystal violet dye from water: adsorption kinetics and isotherm," *Water Treat*, vol. 53, no. 9, pp. 2529–2539, 2015.

[18] Q. Li, Q. Y. Yue, Y. Su, B. Y. Gao, and H. J. Sun, "Equilibrium, thermodynamics and process design to minimize adsorbent amount for the adsorption of acid dyes onto cationic polymer-loaded bentonite," *Chemical Engineering Journal*, vol. 158, no. 3, pp. 489–497, 2010.

[19] S. Beninati, D. Semeraro, and M. Mastragostino, "Adsorption of paracetamol and acetylsalicylic acid onto commercial activated carbons," *Adsorption Science & Technology*, vol. 26, no. 9, pp. 721–734, 2008.

[20] F. J. García-Mateos, R. Ruiz-Rosas, M. D. Marqués, L. M. Cotoruelo, J. Rodríguez-Mirasol, and T. Cordero, "Removal of paracetamol on biomass-derived activated carbon: modeling the fixed bed breakthrough curves using batch adsorption experiments," *Chemical Engineering Journal*, vol. 279, pp. 18–30, 2015.

[21] M. Dutta, U. Das, S. Mondal, S. Bhattachriya, R. Khatun, and R. Bagal, "Adsorption of acetaminophen by using tea waste derived activated carbon," *International Journal of Environmental Sciences*, vol. 6, no. 2, pp. 270–281, 2015.

[22] D. R. Lima, A. Hosseini-Bandegharaei, P. S. Thue et al., "Efficient acetaminophen removal from water and hospital effluents treatment by activated carbons derived from Brazil nutshells," *Colloids and Surfaces A: Physicochemical and Engineering Aspects*, vol. 583, article 123966, 2019.

[23] C. M. Kerkhoff, K. d. Boit Martinello, D. S. P. Franco et al., "Adsorption of ketoprofen and paracetamol and treatment of a synthetic mixture by novel porous carbon derived from *Butia capitata* endocarp," *Journal of Molecular Liquids*, vol. 339, article 117184, 2021.

[24] A. F. M. Streit, G. C. Collazzo, S. P. Druzian et al., "Adsorption of ibuprofen, ketoprofen, and paracetamol onto activated carbon prepared from effluent treatment plant sludge of the beverage industry," *Chemosphere*, vol. 262, article 128322, 2021.

[25] A. L. Bursztyn Fuentes, D. E. Benito, M. L. Montes, A. N. Scian, and M. B. Lombardi, "Paracetamol and ibuprofen removal from aqueous phase using a ceramic-derived activated carbon," *Arabian Journal for Science and Engineering*, vol. 48, no. 1, pp. 525–537, 2023.

[26] M. Sajid, S. Bari, M. S. U. Rehman, M. Ashfaq, Y. Guoliang, and G. Mustafa, "Adsorption characteristics of paracetamol removal onto activated carbon prepared from *Cannabis sativum Hemp*," *Alexandria Engineering Journal*, vol. 61, no. 9, pp. 7203–7212, 2022.

[27] C. Yanan, Z. Srour, J. Ali et al., "Adsorption of paracetamol and ketoprofenon activated charcoal prepared from the residue of the fruit of *Butiacapitate*: experiments and theoretical interpretations," *Chemical Engineering Journal*, vol. 454, article 139943, 2023.

[28] P. V. Nidheesh, R. Gandhimathi, S. Ramesh, and T. Singh, "Adsorption and desorption characteristics of crystal violet in bottom ash column," *Journal of Urban and Environmental Engineering*, vol. 6, no. 1, pp. 18–29, 2012.